Scour Prediction in Cohesive Marine Soils: A Hybrid Approach

John M. Harris, *Director of Research and Innovation, HR Wallingford, Howbery Park, Wallingford, Oxfordshire, OX10 8BA UK; email: j.harris@hrwallingford.com*
Nick Tavouktsoglou, *Senior Engineer, HR Wallingford, Howbery Park, Wallingford, Oxfordshire, OX10 8BA UK; email: n.tavouktsoglou@hrwallingford.com*
Amelia Couldrey, *Senior Scientist, HR Wallingford, Howbery Park, Wallingford, Oxfordshire, OX10 8BA UK; email: a.couldrey@hrwallingford.com*
Richard J.S. Whitehouse, *Chief Technical Director, HR Wallingford, Howbery Park, Wallingford, Oxfordshire, OX10 8BA UK; email: r.whitehouse@hrwallingford.com*
Jamie Klapper, *Design Manager, ScottishPower Renewables, Offshore Business – Project Services, 1 Tudor Street, London, EC4Y 0AH UK; email: jklapper@scottishpower.com*

ABSTRACT: *Regardless of the advancement in scour research in the last three decades, scour prediction at offshore foundations in cohesive and non-uniform soils still involves great uncertainty and remains a challenge for designing structurally efficient and effective foundations offshore. One approach to scour prediction in these marine soils is the application of the Erodibility Index method, allowing for the physical properties of the soil to be considered. The method does not directly take into account the chemical properties of the material, although the mass strength number, M_S, represents the relative influence of chemical bonding properties of the soil through the unconfined compressive strength. This paper presents a case study for a planned offshore wind farm located in the Baltic Sea. The soils in the upper seabed have extremely low to low undrained shear strengths (0 - 15 kPa). The study combines the Erodibility Index method with site-specific geotechnical information and targeted soil sample erosion testing to provide a means of calibrating the method for site-wide use, utilizing the cone penetrometer test data undertaken at every proposed monopile location to enable the Erodibility Index method to be calibrated at each foundation.*

KEYWORDS: Scour, Cohesive, Baltic, Monopile, Erodibility, Probabilistic

SITE LOCATION: Geo-Database

INTRODUCTION

The development of scour in non-uniform, mixed, cohesive soils is still an area of large uncertainty and represents a challenge for designing structurally efficient and effective foundations in the offshore environment. The uncertainty is further complicated by the time-scale required for scour to develop, sediment abrasion effects, and the mechanical effects arising from both pile installation and the operationally- and environmentally-induced dynamic motions of the foundation. With the ongoing rapid growth in offshore wind globally, there is a greater requirement for estimates of scour development in such soils. This is particularly important for large volume serial installation of foundations such as those required for offshore wind farm developments, given that there is a limit to the amount of detailed geotechnical information that can be collected as part of a project, and soil erosion testing—though recommended—is not standard. There is a reliance on geotechnical data, such as undrained shear strength derived from Cone Penetration Tests, supplemented with borehole data collected at a limited number of locations across a wind farm site, combined with laboratory analysis of soil samples. DNV (2021) recommend: "For offshore wind turbines seabed samples should be taken for evaluation of scour potential."

This study aims to demonstrate the benefit of combining field data, laboratory testing, metocean parameters, and empirical prediction methods in developing an enhanced evidence-based set of scour estimates to improve the decision making within

Submitted: 10 June 2022; Published: 28 December 2022
Reference: Harris, J.M., Tavouktsoglou, N., Couldrey, A., Whitehouse, R.J.S., and Klapper, J. (2022). Scour Prediction in Cohesive Marine Soils: A Hybrid Approach. International Journal of Geoengineering Case Histories, Volume 7, Issue 4, pp. 59-75, doi: 10.4417/IJGCH-07-04-06

the project. Whilst the probabilistic approach adopted utilized a correction factor based on a median value, the method could use other percentile values, depending on the risk level deemed acceptable for a given project.

Harris and Whitehouse (2017) presented evidence from both field and laboratory measurements of the scour potential in cohesive soils at monopile foundations and looked at possible approaches to determining scour magnitude in those soils, including hydraulic and mechanical effects. They also stated that scour is a function of both the geotechnical and hydrodynamic processes. Therefore, given the makeup of marine soils, which typically comprise a range of sediments—including sands, gravels, silts, and clays—accurate estimation of scour depth by relatively simplistic empirical equations becomes subject to greater degrees of error depending on the specific soil conditions.

From the compilation of laboratory and field data presented by Harris and Whitehouse (2017), they interpreted the relative importance of the mechanical and erosive contributions. At low values of undrained shear strength, the dimensionless scour depth *S/D*, where *S* is the scour depth at the pile wall and *D* is the pile diameter at mudline, recorded from measurements showed a large range between nearly zero and at least 2 (Figure 1). It was suggested that the large amount of scatter in scour depths observed at low values of undrained shear strength may indicate that in these lower-strength soils, the scour process is influenced more by the soil properties and the hydrodynamic conditions than in higher-strength soils, where it was hypothesized that the scour is controlled more by the soil-structure interaction and the resulting response within the soil matrix than the surface erosion (due to fluid flow). Therefore, in lower-strength cohesive soils there is likely to be more uncertainty in the estimation of scour depth using available predictive methods.

The data in Figure 1 is a revision of the data presented by Harris and Whitehouse (2017) with the same empirical curve (dashed line) bounding the data across the entire range of the dataset. Although the amount of data in the soils with strengths greater than 100 kPa is limited, the reduction in S/D in these stiff soils seems plausible. In the soils with strength less than 100 kPa, whilst the offshore data is limited to S/D values of less than 1—which is still significantly deeper than the >100 kPa range—other data suggests that S/D could exceed 1. Therefore, for soils less than 100 kPa, there is a risk of scour developing to at least 1D and hence a more detailed analysis for projects with soils in this range appears warranted for two reasons: (1) the foundation designer sets a maximum allowable scour depth, and the scour is predicted not to reach this value, or (2) the rate of scour is slow enough that there is time to intervene with mitigation measures during the lifetime of the project.

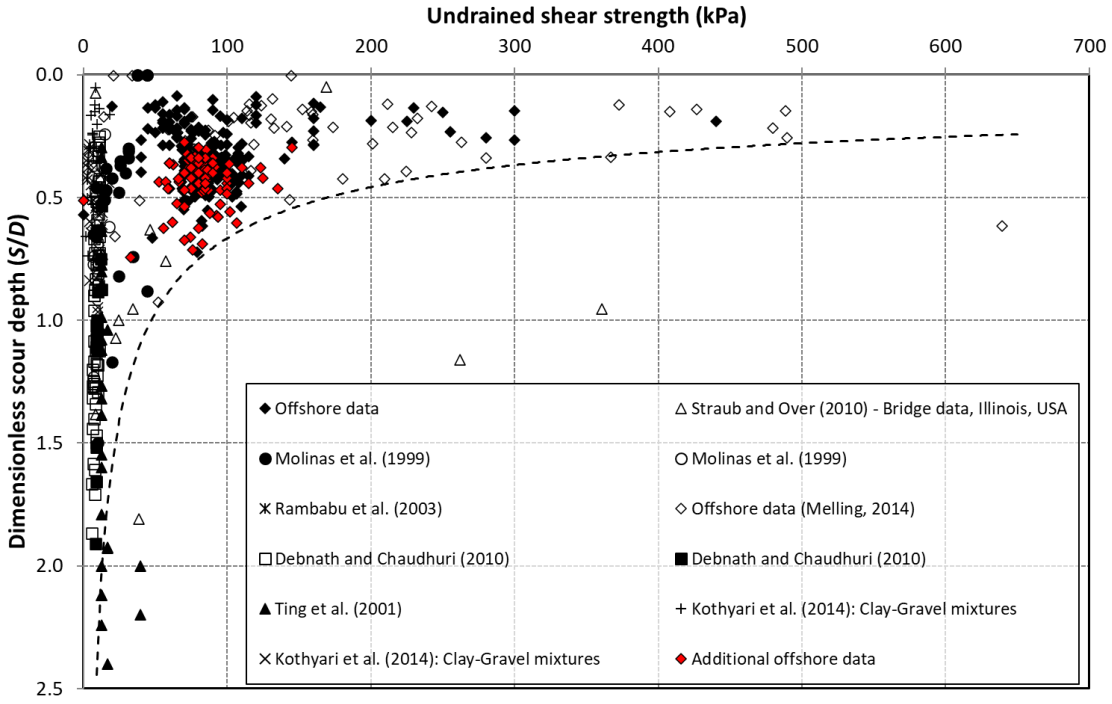

Figure 1. Field and laboratory evidence base of scour depth against undrained shear strength. It should be noted that the data of Ting et al. (2001) is based on generic vane-derived undrained strengths rather than test-specific vane-derived undrained strengths. Modified from Harris and Whitehouse (2017) with additional offshore data.

For offshore wind projects where accurate prediction of the scour depth in cohesive soils can result in significant cost savings (tens of millions UK pounds), adopting a strategy where scour is allowed to develop within the design of the foundation and associated ancillary structures can be beneficial. In offshore locations such as the North Sea and the Baltic Sea, where seabed soil conditions can vary significantly over relatively short horizontal distances, having an accurate estimate of the scour potential is important. In project sites where the soils may comprise weak muds or a mixture of soil types, a more tailored approach to estimating scour depth may be warranted.

In this paper, the authors present a hybrid approach to scour assessment based both on the use of results from experimental soil testing and empirical scour equations. The novelty of the approach is in using the results from the soil testing to calibrate the scour predictions site-wide, based on the testing of soils at locations that provide a good representation of the soil conditions across the site as a whole. The study area is a wind farm within the Baltic Sea where the surficial seabed sediment is comprised of mud overlying a Holocene clay/silt layer with an extremely low to low undrained shear strength (~0 - 15 kPa). Based on the empirical database for scour in Figure 1, the scour in these soils could be appreciable.

The Baltic Sea

The development of offshore wind globally is increasing rapidly, and developments in the Baltic Sea reflect this swift expansion. In September 2020, eight Baltic countries—Germany, Denmark, Poland, Finland, Sweden, Lithuania, Estonia, and Latvia—signed a joint declaration with the European Commission to accelerate the construction of new offshore wind in the region (European Commission website, https://ec.europa.eu/info/news/). Estimates of the future potential for offshore wind in the Baltic Sea suggest more than 90 GW of capacity by 2050.

The Baltic Sea Basin, however, is a highly complex water body, being one of the largest brackish-water inland seas in the world (Rosentau et al., 2017). It is connected to the global ocean system through shallow and narrow straits, receiving a significant volume of freshwater from its drainage catchment. The Baltic Sea is generally quite shallow, with an average depth of about 54 m, and with a maximum depth of about 459 m in the Landsort Deep. It is comprised of several smaller and larger sub-basins. The salinity is variable, being almost freshwater at the easternmost Gulf of Finland and northernmost Bay of Bothnia to about 10‰ at the surface, and 33‰ at the near-bed close to the Danish Straits (Rosentau et al., 2017). In the southwestern Baltic Sea, the Arkona Basin, with a maximum depth of 53 m, and the Bornholm Basin, with a maximum depth of 105 m, have seen some of the larger wind farm developments to date.

The most recent geology of the Baltic, the Quaternary deposits, are comprised mostly of Pleistocene glacial, glacio-fluvial, and lacustrine sediments, in addition to Holocene lacustrine and marine sediments (Rosentau et al., 2017). The thickness of the Pleistocene sediments is variable across the Baltic, with the thinnest deposits (< 10 m) occurring in areas formerly dominated by glacial erosion. Thicker deposits of Pleistocene sediments are observed locally, in areas such as deep tunnel valleys incised in the pre-Quaternary bedrock.

Within the Baltic Sea, the late Pleistocene and Holocene sediment cover and the stratigraphic units are generally formed of three major lithostratigraphic units (Rosentau et al., 2017):

- Brown Baltic clay of glacio-lacustrine origin (Baltic Ice Lake);
- Grey Baltic clay of brackish-water and lacustrine origin (Yoldia Sea and Ancylus Sea); and,
- Olive-grey Baltic mud of marine and brackish-water origin (Littorina and Post-Littorina Sea).

Sedimentation in the Baltic mostly occurs in the deep basins, with regions of mud accumulation located well below the permanent halocline and general depth of wave interaction (Emelyanov and Nielsen, 1995). Sedimentation is dependent on a number of factors including water depth, current speeds, wave conditions, and supply of material.

THE STUDY AREA

Seabed Conditions

The water depths at the wind turbine generator (WTG) locations range between about -40 m and -50 m MSL. The seabed has an average slope of about 0.02º.

On a site-wide scale, the seabed is very smooth with no banks, troughs, sand ridges, or any other large morphological features. Trawl-marks are ubiquitous across the site and are observed at a very high density. The presence of so many of these features, often cut more than 0.2 m into the bed, suggests that the bed does not recover rapidly from mechanical disturbance and that the mud/clay layer is unable to repair itself once disturbed.

There are a few isolated areas of bedforms in the southeast of the site in water depths of less than -41 m MSL that have heights < 0.3 m and wavelengths < 5 m. These bedforms are aligned northeast-southwest and are relatively symmetrical. The bedforms are created in the surface veneer and have both well-formed crests and troughs.

In deeper water (depths greater than -43 m MSL), the bedforms are larger (heights up to 1 m and wavelengths of 40 – 50 m). When compared with the ambient bed level, these features appear not to have formed troughs and have the appearance of bedforms located in an area with a limited supply of mobile sediment, forming only crests out of the available loose (non-cohesive) material. The crests are orientated with their steeper faces toward the south-southeast. Interestingly, these bedforms do not appear to have infilled any of the trawl-mark features and so it seems that they do not interact with the features cut into the clay layer below.

Cone Penetration Tests (CPTs) have been undertaken at all WTG locations. The surficial sediment at the foundation locations is comprised Marine Mud (clay, very silty, organic, very soft, thinly laminated), varying in thickness between 2.2 m to 7.8 m. The thickness of this layer increases from the shallowest part of the site toward the deepest. This soil has an extremely low undrained shear strength, with typical values between about 0 and 15 kPa, and classifies as very soft.

The percentage clay contribution in the Marine Mud layer has been estimated for each WTG location from the PSD samples. On average, the contribution is about 17%, whilst typically the contribution ranges between about 10% and 24%. The percentage clay content was also observed to increase from 14% on average at the surface to 28% at a depth of 4.5 m below the surface, when still within the Mud layer (Figure 2). There was no discernible spatial trend for more or less clay within this layer across the site. The lack of any trend in surface composition was supported by the relatively homogeneous backscatter surface for the site. In terms of clay contribution, the average Mud profile is taken to be representative across the site.

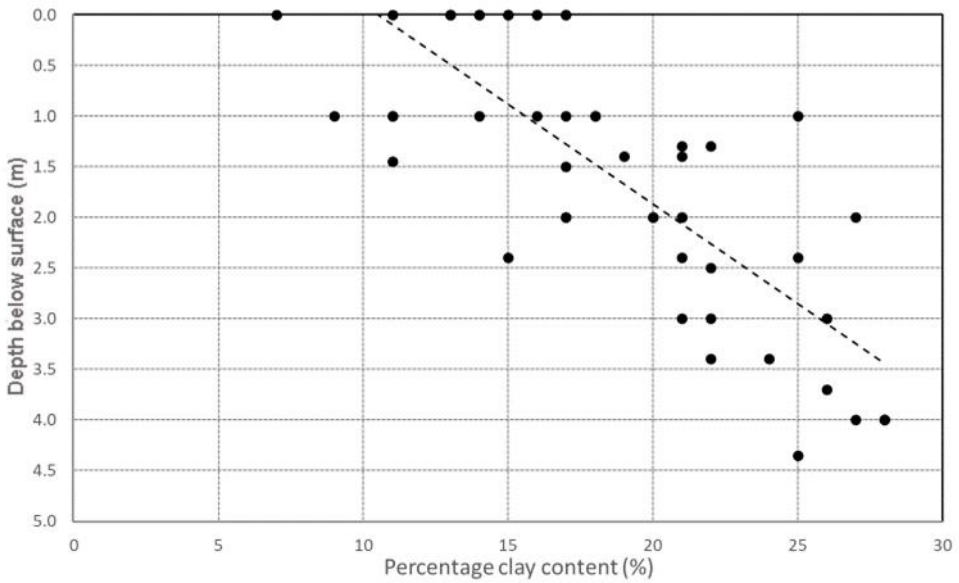

Figure 2. Profile of percentage clay in mud layer.

The d_{10} and d_{60} percentile grain sizes for the Marine Mud range between < 0.002 mm – 0.0045 mm and 0.002 mm – 0.05 mm, respectively. The average median grain size, d_{50}, for the Marine Mud layer is approximately 0.015 mm (medium silt), whilst the 95th percentile grain size, d_{95}, is approximately 0.04 mm (coarse silt). The Marine Mud classification is given in Table 1, whilst Table 2 summarizes the associated values.

Beneath this layer is a Holocene clay/silt layer (clay very silty to silty), with a minimum thickness of 5.00 m toward the southeast of the site and a maximum thickness of 21.8 m at the west of the site. This soil has an extremely low to low undrained shear strength. The Holocene clay/silt classification is given in Table 3, whilst Table 4 summarizes the associated values. The d_{10} and d_{60} percentile grain sizes for the Holocene clay/silt range between < 0.002 mm – 0.008 mm and < 0.002 mm – 0.1 mm, respectively.

Table 1. Marine Mud classification.

Soil description:	Sandy to clayey silt, silty clay
Soil type acc. DIN 4022:	T, U, f_s
Soil group acc. to DIN 18196:	TL, TM, TA
Strength acc. to DIN EN ISO 14688-2:	Extremely low
Consistency:	Liquid to very soft
Degree of overconsolidation:	Normally consolidated
Sensitivity:	Medium sensitive

Table 2. Summary of Marine Mud classification.

Properties of Marine Mud	Unit	Standard deviation	Range		Mean value
			min	max	
Solid density, ρ_s	g/cm^3	0.084	2.34	2.74	2.54
Liquid limit, w_L	%	44.50	27.40	208.80	129.75
Plasticity index, I_p	%	34.51	7.40	157.50	90.55
Consistency, I_c	-	0.281	-1.41	0.30	-0.1
Water content, w	%	56.187	7.20	509.5	140.87
Effective unit weight, γ'	kN/m^3	2.014	0.29	10.99	4.19

Table 3. Holocene Clay/Silt classification.

Soil description:	Sandy Clay/Silt
Soil type acc. DIN 4022:	T/U, f_s
Soil group acc. to DIN 18196:	TL, TM, TA
Consistency:	Very soft to soft
Degree of overconsolidation:	Normally consolidated
Sensitivity:	Low to medium

Table 4. Summary of Holocene Clay/Silt classification.

Properties of Marine Mud	Unit	Standard deviation	Range		Mean value
			min	max	
Solid density, ρ_s	g/cm^3	0.04	2.52	2.75	2.67
Liquid limit, w_L	%	13.90	23.70	93.90	53.01
Plasticity index, I_p	%	11.52	4.00	67.20	32.16
Consistency, I_c	-	0.264	-0.98	0.9	0.14
Water content, w	%	17.49	2.5	130	48.77
Effective unit weight, γ'	kN/m^3	1.473	2.29	18.59	8.02

The underlying soil unit of Glacial Till in some locations is comprised of medium sand to coarse sand, with an average d_{50} of approximately 0.9 mm and d_{95} of approximately 12 mm. As this layer at shallowest was observed at a depth of 8.8 m below seabed, it was not considered a primary concern with respect to scour—but, if the results of scour analysis in the Marine Mud/Holocene layers extended this deep, it would need to be brought into consideration.

Hydrodynamic Conditions

The Bundesamtes für Seeschifffahrt und Hydrographie (BSH) has several measurement stations in the Baltic, including a semi-submersible buoy located at Arkona Becken within reasonable proximity to the study site. Based on observations at this station, near-bed temperatures range between -0.3 and 16.9 ºC, whilst near-bed salinities range between 7.7 and 24.9 PSU

(based on observations at 5 m above seabed). The minimum and maximum derived water densities for the BSH time-series were 1005.4 and 1008.1 kg/m^3, respectively. These values are similar to the minimum and maximum near-bed densities provided in the Design Basis for the wind farm project, which are 1005.8 and 1017.5 kg/m^3, respectively.

Water Levels

Water levels at the study site have been estimated using a BSH Transition Area model, validated with data from water level time-series. A multiplication factor of 1.05 was applied to the water level prior to the extremes analysis. There is minimal change in water elevation over a tidal cycle at the study site, with a tidal range of about 0.09 m under normal tidal conditions (Table 3).

Table 3. Peak tidal levels.

Level	Elevation relative to MSL (m)
Highest Astronomical Tide (HAT)	0.04
Mean Sea Level (MSL)	0.00
Lowest Astronomical Tide (LAT)	-0.05

Currents

The contribution towards the total current from tidally driven currents is very small. There are three main drivers of circulation within the Baltic Sea: wind driven currents, currents driven by the slope of the sea surface (setup by storms and freshwater inputs), and density gradient driven (thermohaline) currents. The Baltic Sea circulation system is complicated by its morphology, comprising a series of small and shallow basins connected by narrow straits (as noted earlier). The presence of sills and basins influences the circulation, particularly in the lower layer of the water column.

Wind driven currents are of particular importance in the Baltic Sea. Whilst wind driven currents primarily act on the surface waters, these currents drive pressure gradients, which in turn drive deep water circulation. The difference in the driving forces between the surface and deep-water currents has an impact on the variability in these currents. The near-bed currents at the project site tend to be more focused in a single direction (toward east-northeast), whilst the surface layers show a greater spread centered around this direction. There is also less seasonal variability in the near-bed current than observed in the upper water column. The current structure will be analyzed next.

The current profiles obtained from time-series at the BSH Arkona Becken (Figure 3) do not follow the commonly used 1/7th power law (e.g., Soulsby, 1997) throughout the water column, although there is still a shear boundary layer near the seabed. Therefore, a standard 1/7th power law approach cannot be used to determine the depth-averaged current speed for the study site. To overcome this, an equivalent depth-averaged current was obtained from the maximum current at each level (near-surface, 25%, 50%, 75%, and near-bed). The maximum speed for each given level was scaled to the depth-averaged current by using the ratio of current speed at that layer to the depth-averaged value (Table 4).

The highest ratio was taken for all observations at all five water column heights. The maximum value of the ratio multiplied by the extreme current for all layers was taken for each direction. The maximum of all directions was then taken to give the omni-directional extreme depth-averaged current (Table 5). These are given for normal conditions and 1 in 1 year, 1 in 10 year, and 1 in 50 year return period conditions.

Table 4. Ratio of current speed for given layer to the depth-averaged current.

Layer	Near-surface	25%	50%	75%	Near-bed	Depth-averaged
Ratio	0.89	0.90	0.97	0.77	0.78	1.00

Table 5. Normal and extreme depth-averaged current speeds.

	Normal conditions	1 in 1 year	1 in 10 year	1 in 50 year
Depth-averaged current speed (m/s)	0.38 (99% from time-series)	0.60	0.88	1.11

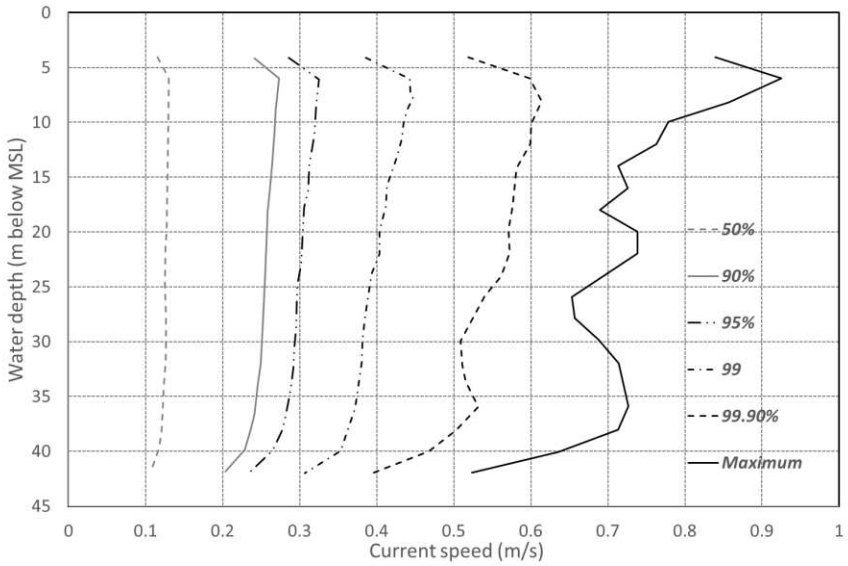

Figure 3. Current speed profile statistics for BSH Arkona Becken time-series data.

Waves

Estimates of extreme wave height and associated peak periods were determined by SPR using a SWAN model, which was validated with data from a number of wave buoys, including the BSH Arkona Becken and FINO2 stations.

A low, central, and high estimate are given for the peak wave period (Table 6). When determining the resultant bed shear stress from the wave height, combined with the lower, central, and higher wave period estimate, it was found that the largest bed shear stress resulted from the higher wave period estimate. Therefore, the higher estimate has been used in the scour calculations.

From the joint occurrence of water levels and wave heights, larger waves are associated typically with slightly higher water levels, although there are also some occurrences of larger waves with lower water levels. Therefore, larger waves can occur with lower water levels, and hence this represents a conservative condition with which to undertake the scour assessment for the study site. Thus, the scour estimates have been determined with the lowest water level for a given return period wave condition.

The misalignment between waves and the currents is on average < 45º. For the purpose of determining the combined near-bed shear stress, it is assumed that the two are co-linear, as this would represent the worst-case scenario.

As no joint probability conditions for waves and currents was available at the time of the study, it was assumed that, although unlikely, the worst case for design would be a combined 1 in 50 year current with a 1 in 50 year wave condition and a 1 in 50 year low still water level.

Table 6: Omni-directional extreme significant wave heights, H_{m0}, and associated peak periods, T_p.

Return period	Wave height (m)	T_p, lower estimate (s)	T_p, central estimate (s)	T_p, upper estimate (s)
1 in 1 year	4.3	8.1	8.5	8.8
1 in 5 year	5.2	8.9	9.3	9.7
1 in 10 year	5.6	9.2	9.6	10.0
1 in 50 year	6.5	9.9	10.3	10.8

Foundations

The design allowed for two different monopile diameters to be used across the site in the shallow and deep-water locations, respectively. However, for the purpose of estimating the maximum scour depth at each WTG foundation location, the

largest pile diameter (i.e., corresponding to the deep-water locations) was applied: 9.0 m. A summary of the design requirements for the monopile foundations is provided in Table 7. Marine growth was also considered in the scour assessment. The fully developed marine growth thickness was estimated to be 100 mm.

Table 7. Foundation design requirements.

Characteristic	Value
Water depth	-40.30 m MSL to -45.80 m MSL
Design life	25 years (+3 years) = 28 years with foundation installed
Clustering strategy	2 clusters with different pile bottom OD (shallow cluster and deep cluster)

SCOUR PREDICTION IN COHESIVE SOILS

Introduction

The prediction of scour in cohesive or multi-modal soils in the sea is complicated. One of the reasons for this is that the scour process is generally much slower in these types of soil, e.g., as compared to uniform sands. As a result, the effect of scour is very much dependent on the design life of the structure(s) *in situ* and the time history of the erosive forces. Harris and Whitehouse (2017) reviewed several approaches, including the method proposed by Annandale (1995). Annandale's approach to estimating the erosion potential of complex soils utilizes the stream power parameter, P, and its relationship to the ability of the soil to resist scour, defined through an Erodibility Index, K. The Erodibility Index provides a measure of the *in-situ* strength of the material, whilst the stream power provides a measure of the rate of energy dissipation in the near-bed region due to hydrodynamic forces. If the locally applied P exceeds the erosion threshold P_R, scouring will occur.

Erosion Testing

HR Wallingford's SedCore erosion rig was used to undertake erosion testing of sediment core samples retrieved from boreholes located across the wind farm. Extracted core samples from the site enabled a selection of the available samples to be chosen for testing. A total of 20 waxed core samples, 300 mm long with an internal diameter of 80 mm, were selected. Core samples were prepared by manually sub-sampling the waxed samples. The cardboard wrapping, wax, foil, and cellophane covering were removed before pushing the stainless-steel sub-sample tube onto the soil sample. Whilst handling was minimized during this process, an element of disturbance was unavoidable.

A detailed view of the central testing duct of the erosion rig and lifting frame for core extrusion is shown in Figure 4. The rig was designed by HR Wallingford to undertake erosion testing of sediment core samples retrieved from site locations. The central testing duct is 0.4 m wide, 0.1 m deep, and 3.0 m long. Water is pumped through the pipework into the duct with cross-section average velocities up to 2.0 m/s being achievable within the rig.

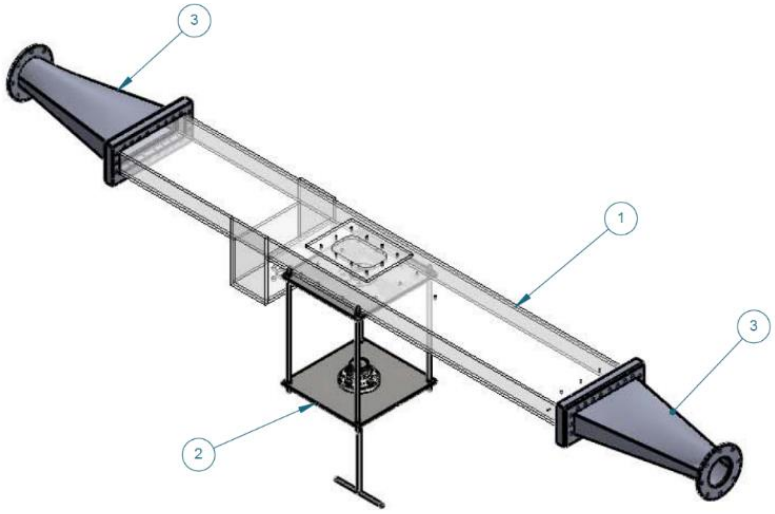

Figure 4. Central testing section of the duct (1), core lifting frame with threaded rod to advance the piston inside the core liner (2), and flow transition pieces (3). Note flow direction is from right to left in the figure.

The erosion testing provides a method of assessing the erodibility of the soils site-wide and providing a means of validating the scour estimates. Based on this information, it was possible to update the estimates based on the results from the erosion tests. During testing, the flow speed was recorded at 10 mm above the duct floor within the central test section. A consistent relationship between flow speed and pump discharge was determined from measurements made before testing commenced (Figure 5).

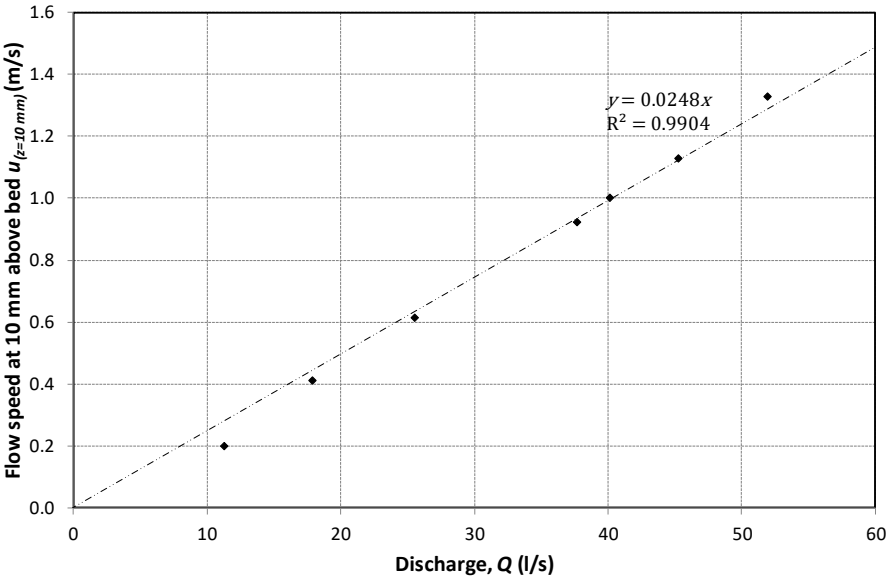

Figure 5. Relationship between pump discharge and reference speed in the duct.

Details of the 20 core samples tested are listed in Table 8, including their depth below the surface (m bbl, meters below bed level).

Table 8. Core samples tested in the erosion rig.

HRW sample number	Depth from (m bbl)	Depth to (m bbl)	Soil layer
HRW06	3.25	3.45	Mud
HRW07	3.25	3.45	Mud
HRW08	2.60	2.80	Clay
HRW09	1.30	1.50	Mud
HRW10	2.25	2.45	Mud
HRW11	3.20	3.40	Mud
HRW12	4.35	4.55	Clay
HRW13	2.60	2.80	Clay
HRW14	2.20	2.40	Clay
HRW15	2.20	2.39	Mud
HRW16	1.40	1.60	Mud
HRW17	1.30	1.50	Mud
HRW18	3.30	3.50	Mud
HRW19	6.40	6.60	Clay
HRW20	3.20	3.40	Mud
HRW21	3.40	3.60	Mud
HRW22	1.50	1.70	Mud
HRW23	3.40	3.60	Mud
HRW24	4.30	4.50	Mud
HRW25	4.60	4.75	Mud

The Marine Mud-Holocene Clay boundary was not always clear cut in the site soil profiles. For example, the transition from one layer to another will not necessarily be registered as a sharp change, with the cone penetrometer resistance influenced by the material ahead and behind the penetrating cone (Treadwell, 1976). Therefore, samples in the Clay immediately below the Marine Mud were considered to be of interest, in addition to those within the Marine Mud, as they may fall within a zone of transition between the two strata. For this reason, samples close to the interface were considered useful to provide information on the erodibility of the material at or just below this interface.

The flow parameters selected for the erosion tests are given in Table 9.

Table 9. Selected test conditions for erosion testing.

Velocity ID	Velocity 0.01 m above bed (m/s)	Discharge Q in rig (l/s)
01	0.2	8.2
02	0.4	16.4
03	0.6	24.6
04	0.9	36.9
05	1.1	45.1
06	1.3	53.3

Each core was subjected to flow conditions in ascending order of flow speed, with the magnitude of erosion measured at each velocity timestep. Once erosion occurred, at least one measurement of the erosion rate was made, depending on the erosion rate and the material left within the core at that velocity step. Each velocity step was held for 10 minutes, or two sets of erosion rate measurements, if erosion rates were negligible. Where available material within the length of the core sample allowed, each sample was subjected to at least one of the overload conditions (U_{mean} = 1.3 m/s).

The erosion rig used freshwater in the tests, and this is considered conservative for testing. The pore water salinity has been known for a long time to influence the attraction between clay particles (Lefebvre et al., 1986) with results showing that for remolded samples with reduced pore water salinity, the soil is more easily eroded. For intact samples, the results showed no difference in erosion properties even after being soaked in distilled water for one week before testing (Lefebvre et al., 1986).

In the present tests, due to the sampling procedure of the soil cores, it was considered that the samples cannot be deemed intact, though nor can they be classed as being remolded. However, the samples are disturbed, both in the initial storage process and through the resampling. Therefore, it is possible that this has made the samples more easily erodible, although it has not been possible to verify this in the current set of tests.

For each flow speed, the erosion rate (if there was erosion observed) was determined from the distance eroded (sample extruded) over a known time interval. These erosion rates were then plotted against flow speed to provide a core-specific erosion profile. For samples where no measurable erosion occurred, a record was made of any particles (number and size) that were eroded at each velocity timestep.

The erosion testing provided a method of assessing the erodibility of the soils site-wide and provided a means of validating the scour estimates. Based on this information, it was possible to update an initial set of scour estimates based on the results from the erosion tests and a strategy to manage the scour put in place.

For example, assuming a wind farm development where monopiles are the selected WTG foundation option and the soil conditions are comprised of cohesive material, a number of possible scour mitigation options exist:

- Scour development can be mitigated within the existing structural design;
- Scour development can be mitigated through extending the monopile embedment length; and,
- Scour development is mitigated through the placement of scour protection.

Let us assume that based on the results of a scour study, it has been determined that the predicted maximum scour depths (derived from a method based on soil strength) are allowable within the design of the foundation and associated structures. As a result of this, the strategy is to allow the scour to develop without the installation of any scour protection. Therefore, monitoring will form a key part in the mitigation strategy to ensure that scouring remains within the design limits.

The erosion testing allowed for the threshold values of shear stress and flow speed to be determined for each core sample tested, and this information was then applied to determine a required stream power for the erosion for each sample. The values of shear stress and flow speed were corrected for the average stickup height of the sample and the corresponding amplification of these parameters. Briaud et al. (2001) carried out studies in their Erosion Function Apparatus (EFA), replacing the soil sample in the Shelby tube by an aluminum cylinder having the same dimensions. Tests were then conducted with no protrusion of the aluminum cylinder, and then with a protrusion equal to 1.2 mm. In both cases, the flow speed in the EFA varied from 0.2 to 5.6 m/s. The results showed that the erosion rate increased with stickup height due to increased shear stresses and flow velocities. Therefore, the average stickup height in the erosion tests was used to correct the applied shear stress and flow velocities to reflect those applied to the sample during testing. The corrections were applied using the Euler number-based method of Tavouktsoglou et al. (2015), where the stickup height and the core diameter were combined to estimate the local increase in shear stress and velocity, and hence stream power. The measured values of required stream power determined from the erosion testing are provided in Table 10.

Table 10. Values of required stream power (threshold values) obtained from the erosion testing.

HRW sample number	Description	Sample depth at top of sample (m bbl)	Required stream power (measured) (W/m^2)	Required stream power (predicted) (W/m^2)
HRW06	Marine Mud to 6.55 m below seabed	3.25	1.91	19.26
HRW07	Marine Mud to 5.30 m below seabed	3.25	1.04	14.38
HRW08	Holocene Clay/Silt from 2.60 m to 14.20 m below seabed	2.60	No value	40.46
HRW09	Marine Mud to 4.20 m below seabed	1.30	2.57	9.04
HRW10	Marine Mud to 4.20 m below seabed	2.25	5.06	10.00
HRW11	Marine Mud to 4.20 m below seabed	3.20	3.98	26.00
HRW12	Holocene Clay/Silt from 4.20 to 17.20 m below seabed	4.35	14.44	32.73
HRW13	Holocene Clay/Silt from 2.50 m to 12.90 m below seabed	2.60	No value	43.84
HRW14	Holocene Clay/Silt from 1.90 m to 9.20 m below seabed	2.20	No value	No value
HRW15	Marine Mud to 2.60 m below seabed	2.20	0.95	1.00
HRW16	Marine Mud to 3.60 m below seabed	1.40	3.62	6.39
HRW17	Marine Mud to 4.50 m below seabed	1.30	6.20	13.04
HRW18	Marine Mud to 5.85 m below seabed	3.30	1.16	25.41
HRW19	Holocene Clay/Silt from 5.85 to 20.40 m below seabed	6.40	5.31	29.90
HRW20	Marine Mud to 4.85 m below seabed	3.20	13.53	16.13
HRW21	Marine Mud to 4.85 m below seabed	3.40	2.57	17.78
HRW22	Marine Mud to 5.80 m below seabed	1.50	4.23	8.68
HRW23	Marine Mud to 5.80 m below seabed	3.40	2.08	19.46
HRW24	Marine Mud to 5.80 m below seabed	4.30	11.95	27.23
HRW25	Marine Mud to 5.80 m below seabed	4.60	No value	23.92

The values of required stream power determined from the erosion testing were compared with the values obtained by applying the approach of Annandale (1995; 2006) using the values of undrained shear strength determined from the CPT measurements corresponding to the sample depth. This provided a set of calculated values of required stream power corresponding to the sample locations, i.e., the predicted values in Table 8. The two sets of values were then compared to determine a correction factor for the predicted stream power value for each sample. Having determined the correction factors for each sample, a cumulative distribution was developed using the top ten values, with the average of the low value cluster of measured values being combined and added as the first point to give the 10^{th} percentile correction value (Figure 6).

From this analysis, lower bound (10^{th} percentile), median, and upper bound (90^{th} percentile) correction values were determined as follows:

- Lower bound correction (10th percentile) = 0.111
- Median correction (50th percentile) = 0.459
- Upper bound correction (90th percentile) = 0.837

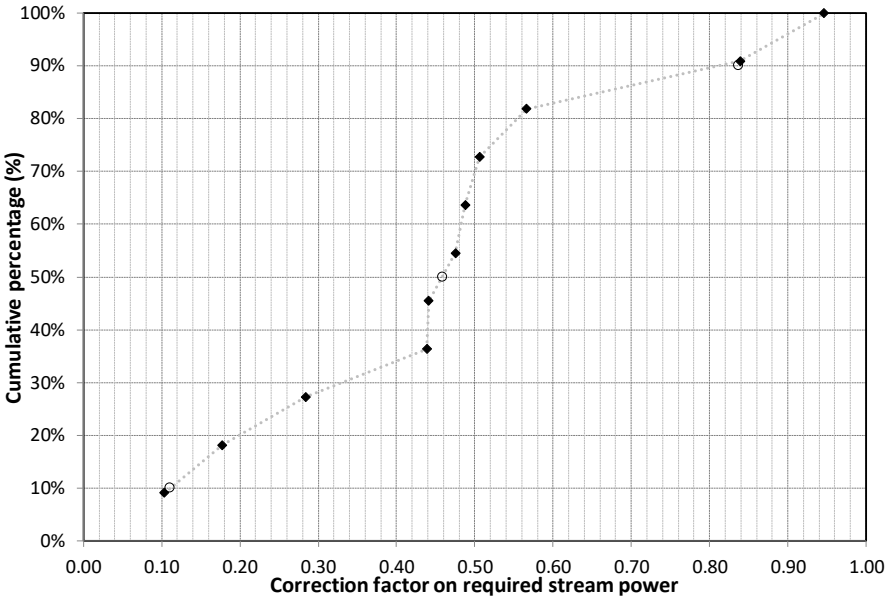

Figure 6. Cumulative distribution for required stream power correction factor. The open circles represent the lower and upper bound percentiles (10th and 90th percentiles, respectively) and the median value.

Using these values, it was possible to recalculate the required stream power for each WTG foundation location based on the undrained shear strengths obtained from the CPT curves. For each location, a lower bound, upper bound, and median curve for the required stream power to erode could then be plotted. For design purposes, the median value is considered appropriate. As an example of the corrected stream power curve, Figure 7 shows the recalculated curve for one of the WTG locations based on the Annandale approach with the measured values obtained from the erosion testing of the samples.

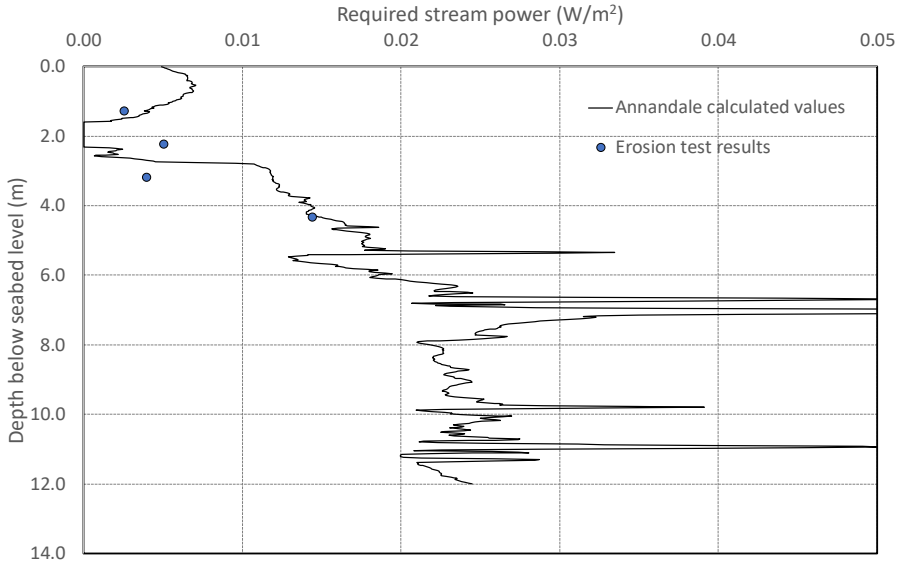

Figure 7. Example of the corrected stream power curve for one of the WTG locations, plotted with required stream power values P_R, corrected with results from erosion testing.

The method of Annandale (1995; 2006) can be applied to consider both the contribution from waves and currents and the soil profile. The original method was applied to scouring around bridge piers, but has been extended for use offshore (e.g., Harris et al. 2010). At the wind farm site, the scour development is current dominated; it is the current-induced scour that will control the maximum scour depth over the design life of the wind turbine foundations. This can be demonstrated through the wave and combined wave and current predictions obtained by applying the methods described in Sumer and Fredsøe (2002). Therefore, the Earth Materials method as applied here has only considered the stream power available at depth through the soil profile from combined wave and currents, and the resistance to erosion in the soil profile uses the undrained shear strength from the CPTs, corrected using the results from the erosion testing.

A subset of 50 foundations were randomly selected from the site and labelled WTG01 through WTG50 for the purposes of reporting within this paper. This method gives a range of scour depth values from 0.2 m to 3.0 m. The results are dependent largely on the profile of the undrained shear strength and the applied correction factor based on the results from the erosion testing (Figure 8). Using this method, the scour depths predicted are typically larger in the west of the site due to the thickness of the Marine Mud layer being greater in this region.

It was observed that, typically, the undrained shear strength of the seabed soils increased from the seabed surface down to 1.5 m below bed and then often decreased again (not as a spike, but more gradually). The implication of this is that if the surface material is lost due to scouring or otherwise weakened, then there is the potential for the scouring to continue to a deeper depth. For this reason, a step change in the predicted scour depths from the 1 in 10 year to the 1 in 50 year conditions were seen, as this small peak in stronger soils is scoured away to reveal the weaker soils beneath. This is an important feature to consider when assessing the scour potential in similar soil conditions, as it has the capacity to increase the scour development and thus the overall scour risk.

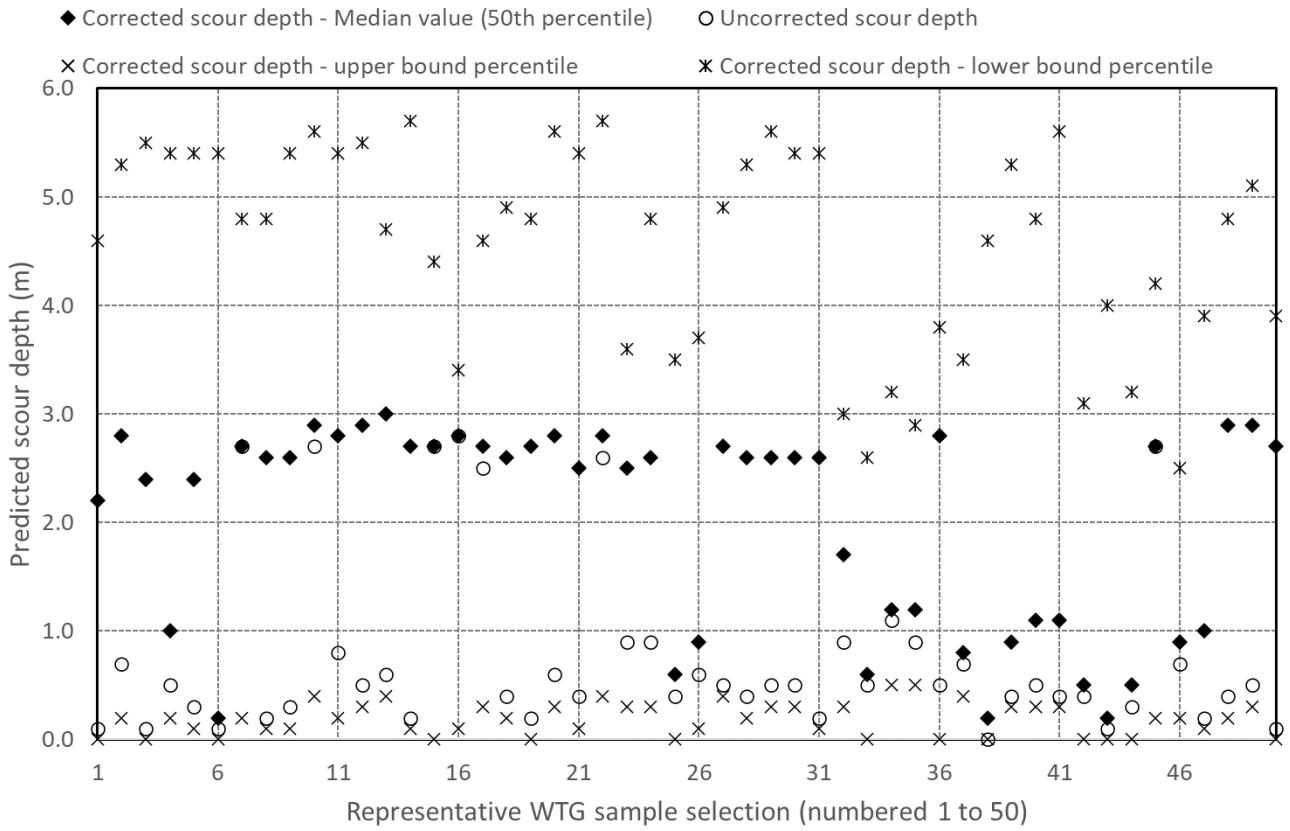

Figure 8. Estimated scour depths at the selected subset of WTG foundations. Plot showing initial predictions based on the Earth Materials approach of Annandale without using the erosion results, together with the erosion test corrected predictions (median value) and the values based on upper and lower limits.

DISCUSSION

The erosion of the samples showed some variability, although the observed erosion at the edges of the samples is likely to be a function of increased turbulence and flow speeds due to the imposed stick-up height during testing, as well as disturbance of the samples during the sub-sampling process. Depending on the composition of the samples, the observed erosion behavior is likely to vary. Debnath and Chaudhuri (2012) noted three different modes of erosion: particle-by-particle, in flocs, and "chunk-by-chunk." A similar observation was made by Kothyari et al. (2014). Mirtskhulava (1966) noted from observations taken using a high-speed camera (3,000 frames per second) the dependency of the erosion of cohesive soils on their composition, structural uniqueness, moisture content, and degree of cohesion. Mirtskhulava also remarked on the force effects of the "pulsating bed flow" and how the coherence between the particles of the soil gets "fatigued" such that erosion occurs when the resultant of the "active forces" exceeds the "passive ones."

Harris and Whitehouse (2017) compared the CPT based (Earth Materials method) predicted and observed values of *S/D* from offshore sites, and on average found the method underpredicted scour depth. Based on this experience, the erosion testing for this study provides a means of calibrating the empirical scour predictor, in this case the Earth Materials method, based on the erodibility of soils collected directly from the site. It was not possible to apply individual correction values at each WTG foundation, as this would require erosion testing of the soils at every foundation and with depth up to the expected maximum scour depth. Therefore, it was necessary to develop a probabilistic approach based on the samples tested.

Having determined the correction factors for each sample, a cumulative distribution was developed using the top ten values with the average of the low value cluster added as the first point. This was done to avoid biasing the results with the results from the weaker soils, some of which were only representative of silt/sand pockets within the overall soil profiles. In addition, it was not possible to include results for those higher-strength soils where the erosion was negligible across the range of flow conditions run for.

The cumulative distribution provides the probability (in this instance given as a percentage) that the correction factor on required stream power will take a value less than or equal to that value. Therefore, for example, the 90th percentile value (0.837) implies that 90 percent of the results would be less than or equal to this value.

To obtain site specific estimates of scour, a combined approach of the Earth Materials method to derive P_R, with correction of the P_R using the results from the erosion testing applied in a statistical fashion, yielded the following benefits on the scour predictions for the subset of 50 WTG locations presented in the paper. In the original prediction, 42 of the representative selection of WTG locations had scour depths of < 1 m, whilst in the corrected prediction this reduced to 11 (Table 11). The number of locations in the 2 to 3 m range increased from 7 to 31. The benefit of the erosion testing ensured that the strength of the seabed soils at the wind farm site was not overestimated with respect to erosion resistance, resulting in unconservative scour predictions. The erosion testing also provided a means of calibrating the empirical scour model site-wide, thereby providing confidence in the overall results of the scour assessment without the need to undertake erosion testing at all WTG foundation locations (which would be prohibitive in terms of time and cost).

Table 11. Summary of the differences in scour depth ranges between the uncorrected and corrected required stream power.

Scour depth range (m)	Total number of locations in original prediction	Total number of locations in corrected prediction
< 1 - ≥ 0	42	11
< 2 - ≥ 1	1	7
< 3 - ≥ 2	7	31
< 4 - ≥ 3	0	1
Sum	50	50

The erosion rate is defined by both the flow condition and the soil properties. The duration of the tests will influence the ability to more accurately assess the erosion rate when the sample erodes at a slow or very slow rate. In the present tests, a ten-minute test period was allowed per each flow condition. This equates to a standard assumption for a steady-state flow condition within a time-varying flow for analysis of boundary layer measurements in the sea (Dyer, 1986). This standardization provides inter-comparability between tests/samples, but does not enable a rate of erosion to be determined where the sample does not erode within the allowed time. The practicalities of very slow erosion were recognized by Briaud et al. (1999), who considered the erosion rate to be zero if the erosion rate was less than 1 mm/hr.

The soil samples, whilst aiming to provide site-wide coverage, also demonstrate the variability of the ground conditions. One sample, HRW15 (Figure 7), showed the effect of the sand/silt lens observed in the borehole data, with relatively rapid erosion of this layer until the underlying clay layer was reached in the sample. Therefore, where these sand/silt layers are encountered within a scour profile, they are expected to erode. The occurrence of these thin weaker layers is considered unrepresentative of the soil profile as a whole.

From the erosion testing, there appeared also to be a dependency between the organic content and the erodibility of the sample. Samples having a strong organic odor were found to be more susceptible to erosion than ones without. This is useful information when reviewing the borehole logs for individual WTG locations for identifying those foundations that may be more susceptible to scour.

The results also demonstrate that under typical flow conditions, the erosion rate is generally low. In some instances, only under the more extreme return period conditions was erosion observed (> 0.6 m/s). This again demonstrates the relationship between erosion rate and both the flow condition and the soil properties, and how variability in the vertical soil structure impacts the rate of erosion.

To enable the results from the erosion testing to be applied site-wide, it is important to link them back to the geotechnical data. This has been facilitated through relating the rate of erosion to the value of stream power in order to improve the estimates of scour.

The impact of remolding of the soil by pile installation and deflections during operation was assessed indirectly based on a sensitivity factor derived for the Mud layer at the Offshore Substation (OSS) position. This implied that the shear strength was reduced by a factor of about 3.3; this can be used directly by introducing a reduction in resistance to scour in the Earth Materials method. It should be noted that this sensitivity factor is strictly valid only for the OSS position, but was used to provide an estimate as to the potential impact of remolding at the WTG positions. Table 12 provides a summary of the change in scour depth range due to the estimated impact of remolding.

Table 12. Summary of the change in scour depth range due to the estimated effect of remolding.

Scour depth range (m)	Total number of locations in reduced shear strength factor of 3.3
< 1 - ≥ 0	0
< 2 - ≥ 1	1
< 3 - ≥ 2	17
< 4 - ≥ 3	32
Sum	50

CONCLUSION

The very soft cohesive soils at this case study site in the Baltic Sea lie within a range that scour is expected to occur, and the estimates needed to be constrained. The results of a combined analysis using the Earth Materials approach, to derive soil resistance to scour informed by erosion testing of field cores, has led to a balanced set of maximum scour depth estimates. The main conclusions from the erosion tests are summarized as follows:

- 20% of the tested samples did not erode at all over the range of flow velocities selected within the allowed time-scale. Whilst the majority of these samples were within the Holocene clay layer, one sample within the Marine Mud layer, HRW25 also did not erode. It was noted that from the borehole records for this sample the soil behavior type classification of “clay” was the same as the clay classification for the Holocene layer. Therefore, the similarity in erosion behavior is justifiable.

- 70% of the tested samples required a mean flow velocity measured very near the bed greater than 0.6 m/s to initiate erosion. This speed only occurs in the more extreme current conditions (Figure 3).

- The results of the erosion tests for samples coming from the same boreholes showed that there was a weak dependency between depth and erodibility, with deeper samples showing smaller erodibility than shallower samples.

- There appeared to be a dependency between the organic content and the erodibility of the sample. Samples having strong organic odor were found to be more susceptible to erosion than ones without.

- The values of required stream power determined from the erosion testing were compared with the values obtained by applying the Earth Materials approach of Annandale (1995; 2006), using the values of undrained shear strength determined from the CPT measurements. A weak positive relationship was observed. The predicted CPT stream powers were always larger than the erosion testing derived values. This meant that the scour analysis would have underestimated the depth of scour.

- The testing results have shown that the Holocene Clay layer (Sandy Clay/Silt) is more resistant to erosion than the Marine Mud (sandy to clayey silt, silty clay) layer. The erosion surfaces formed are irregular in the Mud and Clay, and the edges of some Clay samples are smoothed by the force of the flow; this has been interpreted as indicating that, in the long-term, very slow erosion of exposed Clay surfaces might take place under typical flow conditions. Under higher return period events, the erosion rates are expected to increase—except in the stiffer clays where the erosion testing showed negligible erosion to occur; these are predominantly in the Holocene Clays. The testing results showed the main scour risk was confirmed as being in the Marine Mud layer, and this was used to inform further analysis.

The knowledge gained from the erosion tests and interpretation of the site geotechnical data and metocean parameters allowed an improved evidence-based set of scour estimates to be made, which benefited the project.

ACKNOWLEDGMENTS

We are grateful for access to data provided to us by the client, and for allowing us permission to present the data in this paper. HR Wallingford authors were funded by their strategic scour research program whilst preparing the paper.

REFERENCES

Annandale, G.W. (1995). "Erodibility." *Journal of Hydraulic Research*, 33(4), 471-494.

Annandale, G.W. (2006). *Scour Technology: Mechanics and Engineering Practice*, McGraw-Hill, New York.

Briaud, J.-L., Ting, F.C.K., Chen, H.C., Cao, Y., Han, S.W. and Kwak, K.W. (2001). "Erosion function apparatus for scour rate predictions." *Journal of Geotechnical and Geoenvironmental Engineering*,127, 105-113.

Briaud, J-L., Ting, C.K., Chen, H.C., Gudavalli, R., Perugu, S. and Wei, G. (1999). "SRICOS: Prediction of scour rate in cohesive soils at bridge piers." *Journal of Geotechnical and Geoenvironmental Engineering*, 125(4), 237-246.

Debnath, K. and Chaudhuri, S. (2012). "Local scour around non-circular piers in clay-sand mixed cohesive sediment beds." *Engineering Geology*, 151, 1-14.

DNV (2021). *Support structures for wind turbines*. DNV-ST-0126, Edition December, 228.

Dyer, K.R. (1986). *Coastal and Estuarine Sediment Dynamics*, Wiley-Interscience.

Emelyanov, E.M. and Nielsen, O.B. (1995). "Types and composition of bottom sediments (O-3 cm)." *Aarhus Geosci,*. 5, 127-139.

Harris, J.M. and Whitehouse, R.J.S. (2017). "A review of scour development around large diameter monopiles in cohesive soils: Evidence from the field." *J. Waterway, Port, Coastal, Ocean Eng.*, 143(5).

Harris, J.M, Whitehouse, R.J.S. and Sutherland, J. (2010). "Scour Assessment in Complex Marine Soils – An Evaluation through Case Examples." *Proc. of the Fifth International Conference on Scour and Erosion (ICSE-5)*, (eds.) Burns, S.E., Bhatia, S.K., Avila, C.M.C., and Hunt, B.E., Holiday Inn Golden Gateway, San Francisco, California, Nov. 7 -10, ASCE, Geotechnical special publication No. 210, 450 - 459.

Kothyari, U.C., Kumar, A. and Jain, R.K. (2014). "Influence of cohesion on river bed scour in the wake region of piers." *Journal of Hydraulic Engineering*, 140(1), 1-13.

Lefebvre, G., Rohan, K. and Milette, J-P. (1986). "Erosivity of intact clay: Influence of the natural structure." *Can. Geotech. J.*, 23, 427-434.

Mirtskhulava, Ts.E.(1966). "Erosional stability of cohesive soils." *Journal of Hydraulic Research*, 4(1), 37-50.

Rosentau, A., Bennike, O., Uścinowicz, S. and Miotk-Szpiganowicz, G. (2017). "The Baltic Sea basin." Chapter 5, *In: Submerged landscapes of the European continental shelf, (eds.) Flemming, N.C., Harff, J., Moura, D., Burgess, A. and Bailey, G.N., John Wiley & Sons Ltd*, 103 – 133.

Soulsby, R.L. (1997). *Dynamics of marine sands: A manual for practical applications*, Thomas Telford Publications, London.

Tavouktsoglou, N.S., Simons, R.R., Whitehouse, R.J.S. and Harris, J.M. (2015). "Bed shear stress distribution around offshore gravity foundations." *Proc. of the ASME 2015 34th International Conference on Ocean, Offshore and Arctic Engineering*, OMAE2015, St. John's Newfoundland, Canada, Paper No. OMAE2015-41966.

Treadwell, D. D. (1976). *The influence of gravity, prestress, compressibility and layering on soil resistance to static penetration,* PhD thesis, Univ. of California, Berkeley.

NOTATIONS

BBL – Below Bed Level
BSH – Bundesamtes für Seeschifffahrt und Hydrographie
CPT – Cone Penetration Test
EFA – Erosion Function Apparatus
f_s – Fine sand
HAT – Highest Astronomical Tide
LAT – Lowest Astronomical Tide
MP – Monopile
MSL – Mean Sea Level
OD – Outer diameter
OSS – Offshore Substation
PSD – Particle Size Distribution
PSU – Practical Salinity Units
SPR – ScottishPower Renewables
SWAN – Simulating WAves Nearshore numerical wave model
T – Clay
TA – High plasticity clay
TL – Low plasticity clay
TM – Medium plasticity clay
TP – Transition Piece
U – Silt
WTG – Wind Turbine Generator

The open access Mission of the International Journal of Geoengineering Case Histories is made possible by the support of the following organizations:

Access the content of the ISSMGE International Journal of Geoengineering Case Histories at:
https://www.geocasehistoriesjournal.org